This is a preprint, the final version is subject to change, of the American Mineralogist (MSA)
Cite as Authors (Year) Title. American Mineralogist, in press.
(DOI will not work until issue is live.) DOI: http://dx.doi.org/10.2138/am-2016-5708

Revision 1

Title: Raman spectroscopy of siderite at high pressure: Evidence for a sharp spin transition.

Authors and affiliation:

Müller Jan[1]

Speziale Sergio[1]

Efthimiopoulos Ilias[1]

Jahn Sandro[2]

Koch-Müller Monika[1]

[1] GFZ, German Research Centre for Geosciences, Telegrafenberg, 14473 Potsdam, Germany [2] University of Cologne, Institute of Geology and Mineralogy, Greinstraße 4-6, 50939 Cologne, Germany

Corresponding Author: Jan Müller, jmueller@gfz-potsdam.de

Abstract

We have measured high-pressure Raman spectra of both siderite single crystalline and polycrystalline powder samples in diamond anvil cell experiments across the pressure induced high spin (HS) to low spin (LS) transition of Fe^{2+}. Between 43.3 and 45.5 GPa we observed a color change from transparent to green, which is associated to the spin transition. Furthermore, we calibrated the position of the Raman active ν_1-mode with pressure. In a second diamond

anvil cell experiment, we observed the color change from transparent to green in the form of a transition front passing through the single crystal and collected Raman spectra across the transition front. We were able to constrain the stress variation across this transition front to about 0.2 GPa, well below the resolution of our Raman-based pressure/stress calibration. In contrast to the single crystal, the powder sample shows the spin transition over a pressure range of 5 GPa, which we attribute to intergranular stresses. We conclude that within the resolution of our stress/pressure calibration the spin transition of iron in single-crystalline siderite is sharp.

Introduction

Carbonates are the most frequent carbon carriers in the Earth's mantle. Therefore their behavior at high pressure promotes our understanding of the processes involved in the deep carbon cycle. Carbonates have been found as inclusions in diamonds, thus proving their existence in Earth's mantle (e.g. Kaminsky 2012). Furthermore, the proof from natural samples is backed by various experimental studies, which show that various carbonates can be stable under mantle conditions. Examples include Merlini et al. (2012) who studied some of the polymorphs of $CaCO_3$ up to 40 GPa and Isshiki et al. (2004) who showed that magnesite is stable up to conditions resembling 2600 km depth in the Earth

It has been shown that the major lower mantle minerals ferropericlase and bridgmanite undergo a pressure induced transition of Fe^{2+} from high spin (HS) to low spin (LS) state (Badro et al. 2003; Lin et al. 2012), which changes the physical and chemical behavior of theses minerals in terms of e.g. sound velocities and thermal conductivities (e.g. Lin et al. 2013).

A spin transition at high pressure can also be expected in Fe^{2+} bearing carbonates. Therefore, either the pure endmember siderite ($FeCO_3$), or Fe-rich magnesite ($MgCO_3$), rhodochrosite ($MnCO_3$), and calcite ($CaCO_3$) are the ideal materials to study the fine details of such effect on carbonates (e.g. Lavina et al. 2010; Liu et al. 2014). In the following paragraphs we refer to both the siderite endmember and siderite solid solutions as siderite.

Siderite crystalizes in the calcite structure at ambient conditions. It has been shown by single crystal x-ray diffraction (XRD) at high pressure that a sharp and isostructural volume collapse ranging from 6.5 to 10 % (Lavina et al. 2009, 2010; Nagai et al. 2010; Farfan et al. 2012) takes place between 40 and 50 GPa depending on the composition of siderite (Tab. 1). The volume collapse is assigned to the HS to LS electronic transition of the octahedrally coordinated Fe^{2+} in siderite. The phenomenon is also accompanied by a sudden change of color from transparent to green (e.g. Lobanov et al. 2015). Depending on the experimental methods and the exact composition of the sample material (Tab. 1), however, a general inconsistency about the exact pressure and, especially, about the pressure range of the spin transition exists. Studies that used Raman spectroscopy place the spin transition over a sizeable pressure range (4 – 7 GPa), where the two configurations are thought coexist as micro-domains (Spivak et al. 2014; Cerantola et al. 2015). On the contrary, single crystal XRD studies observe a sharp spin transition (1 – 2 GPa).

Lavina et al. (2010), who performed single crystal XRD on siderite, observe the coexistence of HS and LS state within a narrow pressure range, which they interpret as measuring both HS and LS domains in their sample. A similar behavior was observed in a single-crystal optical absorption study (Lobanov et al. 2015). In particular, Lobanov et al. (2015) report the appearance of a green (LS) domain progressively extending to the whole sample at the

expense of the original (HS) transparent domain between 44 and 45 GPa and propose that a stress gradient is responsible for the coexistence of both HS and LS configurations. Domains of high-pressure phases passing through the low-pressure phase have been previously observed. For example Arlt & Angel (2000) see the phase transition of spodumene from the $P2_1/c$ structure to the $C2/c$ structure in the form of a transient domain progressing through a single crystal.

In order to understand whether the spin transition in siderite is sharp or broad, and in order to probe its sensitivity against pressure gradients in the sample, we have performed both single-crystal and powder Raman spectroscopic measurements at high pressures. Our experimental approach is distinct in that we were able to quantify the stress state across a transition front in a siderite single crystal by taking advantage of the high spectral and spatial resolution of micro-Raman technique. This approach gives a superior evaluation of the stress state in the sample, because ruby and other pressure sensors are always placed away from the sample, thus not giving direct information about the stress state on the sample. We conclude that the spin transition takes place in a pressure range less than 1 GPa, comparable with the resolution of our stress calibration.

Methods

As a starting material we used both natural and synthetic siderite samples of two compositions. The natural siderite was chemically homogeneous (Fig. 1) and has the composition of approximately $Fe_{0.89}Mn_{0.07}Mg_{0.03}Ca_{0.01}CO_3$, which was determined at GFZ Potsdam with a Carl Zeiss SMT Ultra 55 Plus scanning electron microscope equipped with a Tungsten-zircon field-emission filament. The natural siderite single crystal was chosen in

93 order to have a large enough size that can be mapped using Raman spectroscopy. The crystals
94 of this sample were polished from both sides to a thickness of 20 μm. Synthetic $FeCO_3$ powder
95 was synthesized following French (1971) and a film of the material was prepared by squeezing
96 the powder in a diamond anvil cell without gasket to a thickness of 10 to 20 μm.
97 Two diamond anvil cell experiments were performed. The first experiment was done in a
98 Boehler-Almax-cell (Boehler, 2006) containing a 30 x 30 μm^2 large natural crystal. It was
99 loaded with Neon at the Goethe University Frankfurt. This experiment will be referred to as
100 DAC-N. Raman spectra for DAC-N were measured with a HORIBA Jobin Yvon LabRAM
101 HR800 UV-VIS spectrometer equipped with a 514.5 nm Ar^+-laser. The measurements were
102 performed in the spectral range between 200 and 1250 cm^{-1}, and each measurement lasted 30 s
103 with 10 accumulations.
104 The second experiment was performed in a piston-cylinder Mao-type DAC, containing a 50 x
105 30 μm^2 large natural crystal plus the synthetic siderite film and was cryogenically loaded with
106 liquid argon. This experiment will be referred to as DAC-A. Raman spectra in experiment
107 DAC-A were measured with a HORIBA Jobin Yvon LabRAM HR800 VIS spectrometer with
108 a blue (473 nm) diode pumped solid-state laser. Measurements were done between 200 and
109 1250 cm^{-1} or 1000 and 1250 cm^{-1} and lasted for 40 s with 5 accumulations.
110 In both experiments we used a 50x lens. To determine the spatial resolution in the DAC we
111 measured the amplitude of a Raman active mode with respect to the position in the DAC,
112 thereby crossing over the edge of the single crystal. The position dependence of the amplitude
113 can be fitted with a sigmoidal function, whose derivative is a peak-shaped curve (Fig. 2). The
114 FWHM of this curve is then defined as the spatial resolution of 9±1 μm.

The diamond anvil cells were equipped with either type I (DAC-N) or type II (DAC-A) diamonds of 300 μm culet and Rhenium gaskets, which where preindented between to a thickness of 30 to 40 μm. The holes in the gaskets were 130 μm in diameter. Furthermore, ruby crystals were loaded in each cell in order to determine the pressure using the ruby fluorescence method after Mao et al. (1986). In the DAC-A experiment the rubies were nearly 20 to 30 μm in diameter and thus, in principle, too large for the setup. As a consequence the rubies bridged the two culets and were stressed and one ruby even crashed during loading. For pressure determination the smaller fragments were used. Thus, the pressure determined by ruby was different than the pressure on the samples. Further remarks about the rubies in DAC-A are found in the discussion. In DAC-N two rubies were loaded with only 5 and 15 μm in diameter. We used only the smaller ruby for pressure measurement, since it is less susceptible to stress heterogeneity in the sample chamber. To measure the ruby fluorescence after each pressure increase we used the Raman system. In experiment DAC-A the measurements were done several hours after each pressure increase in order to equilibrate the system, whereas in experiment DAC-N we waited for only 30 to 60 minutes. Klotz et al. (2009) report a standard deviation for ruby fluorescence measurements in argon as pressure transmitting medium of 1.2 GPa at 40 GPa and 0.3 GPa at 40 GPa for neon as pressure transmitting medium. The uncertainty of the pressure value for experiment DAC-A is estimated to be ± 2 GPa.

Results

At ambient pressure five distinctive peaks are observable in the siderite single crystal spectrum between 200 and 2000 cm^{-1} (Fig. 3). These modes are assigned to the lattice modes libration (L) and translation (T), the internal vibrations of the CO_3^{2-} group (ν_4, ν_1,) and the

combination band of the ν_1- and ν_4-mode (Rutt and Nicola 1974). A broad band at approximately 500 to 600 cm^{-1} is thought to be caused by Fe^{2+} electronic excitation, and at 1530 cm^{-1} an unassigned band is observed (Langille and O'Shea 1977). In all spectra of the siderite film a broad band is visible at around 760-770 cm^{-1}, which comes from the background.

In experiment DAC-N we measured Raman spectra of the sample up to 63 GPa (Fig. 4). Up to 41.7 GPa all modes (L, T, ν_4 and ν_1) are shifted to higher wavenumbers with increasing pressure. Between 43.3 and 45.5 GPa we observe a sudden frequency change of all modes as a consequence of the spin transition. Both of the L and T modes jump to higher wavenumbers because of the distance reduction between the CO_3^{2-}-groups and the cations (Lavina et al. 2010; Farfan et al. 2012; Cerantola et al. 2015). The ν_4-mode as well jumps to higher wavenumbers due to a decrease of the O-O bond lengths (Lavina et al. 2010; Cerantola et al. 2015). Contrary to the other modes the ν_1-mode is shifted to lower wavenumbers between 43.3 and 45.5 GPa caused by an increase of C-O bond lengths after the spin transition (Lavina et al. 2010). At 43.3 GPa the ν_1-mode shows a small shoulder on the left side, which is assigned to the first occurring LS state and at 45.5 GPa the ν_1-mode shows a small shoulder on the right side, which is assigned to the last remaining HS state. The color of the crystal also changes from transparent to green (Fig. 5), which is due to the spin transition. We do not observe a transition front as in the study by Lobanov et al. (2015) because of a large pressure step. Fig. 6 shows a linear fit of the ν_1-mode in experiment DAC-N. As the ν_1-mode is the most intense mode in the siderite spectrum, this band is the best candidate to calibrate the peak position against pressure. For the HS-mode the fit function

$$R_{HS} = 2.2\ (\pm 0.1) * P + 1091.7\ (\pm 3.1)$$

and for the LS-mode the fit function

$$R_{LS} = 1.5\ (\pm 0.1) * P + 1089.3\ (\pm 5.6)$$

is obtained with R_{HS} or R_{LS} being the Raman shift in cm^{-1} and P being the pressure in GPa under nearly hydrostatic conditions. Cerantola et al. (2015) report slopes of 2.17 cm^{-1}/GPa (HS) and 1.6 cm^{-1}/GPa (LS) and are fairly good agreement with our slopes of 2.207 cm^{-1}/GPa (HS) and 1.528 cm^{-1}/GPa (LS).

In the high-pressure Raman spectra taken on the siderite film (DAC-A), only the ν_1-mode could be followed at all pressures (Fig. 7). At around 42.8 GPa a new peak appears next to the ν_1-mode at lower wavenumbers, which increases in intensity with increasing pressure at the cost of the old ν_1-mode. The change of the ν_1-mode and the occurrence of a new mode indicate the spin transition and the two bands are assigned to the HS ν_1-mode and the new LS ν_1-mode (Spivak et al. 2014, Cerantola et al. 2015). Furthermore, the spin transition is indicated by the appearance of two new peaks at 46.4 GPa, which are assigned to the T-mode and the ν_4-mode. Overall the spin transition in the siderite film occurrs in a pressure range of 4 to 5 GPa, which is in accordance to the single crystal results of Cerantola et al. (2015).

The single crystal Raman spectra (Fig. 8) taken within the same experiment (DAC-A) show the L, T and ν_4-modes more clearly. With increasing pressure all modes shift continuously to higher wavenumbers. From 47 to 49.7 GPa a discontinuous jump of the L, T and ν_4-modes to higher wavenumbers is observable. The ν_1-mode again jumps to lower wavenumbers (Fig. 8) and the spectra do not show the HS and LS ν_1-mode simultaneously at the same pressure, as it was observed in the spectra of the siderite film. Again we assign the mode at 47 GPa and 1182

180 cm^{-1} to the HS ν_1-mode and that at 49.7 GPa and 1153 cm^{-1} to the LS ν_1-mode. With further
181 increasing pressure the LS modes shift to higher wavenumbers (Fig. 9).
182 In experiment DAC-A we again observed the color change from transparent (HS) to green
183 (LS) in the single crystal during compression, but the pressure steps were too large to observe
184 the transition front. Thus, the sample was slightly decompressed and we managed to obtain the
185 transition front at 45 GPa (Fig. 10). We then collected Raman spectra across the transition
186 front. The sample was further decompressed to HS conditions, and carefully compressed
187 again. We then observed the transition front under compression. This compression and
188 decompression process was done several times, resulting in an increased pressure range of the
189 spin transition. We attribute this transition pressure range increase to the fracturing of the
190 single crystal, thus behaving similar to the siderite film.
191 On the left side of the transition front (Fig. 10), the transparent color was assigned to HS-
192 siderite and the green color on the right side to the LS-siderite. Eight Raman spectra of the ν_1-
193 mode were taken along the transition front (Fig. 11) and the respective spectra are shown in
194 (Fig. 12). For convenience, we assumed that the scattering volume at each measurement point
195 had a cylindrical shape. The distance between each point is 4 to 5 μm. Because of the spatial
196 resolution of 9 μm, the scattering volume sampled at each measurement was likely to overlap
197 with the next and the previous point and, therefore, the obtained signal was mixed. Point 3 was
198 measured on the LS side and is the first point that showed a small signal of HS, which must
199 have come from point 4 since the scattering volume probed at point 2 was completely LS. On
200 the other side point 7 was measured on the HS side and was the first point that got a small
201 signal of LS, which must have come from point 6. Therefore we were able to track down the

transition front between point 4 and 6 to a width of 10 - 15 µm. Overall no large shift of the ν_1–mode was observed, therefore ruling out a large stress gradient.

In Tab. 2 the peak positions of the respective spectra from Fig. 12 are found, together with their calculated pressures changes. We were not able to fit the HS ν_1-mode for point 1 and 2 and for point 8 the LS ν_1-mode. The overall calculated pressure gradient is not larger than 2 GPa. From point 1 to 2 the pressure calculated by R_{LS} drops over 1 GPa. Since point 1 was measured close to the gasket it might be that the gasket was pressing on the crystal. Thus, the LS siderite was found at the right side of the crystal even though the highest pressure would be expected in the center of the sample chamber. From the former analyses the transition front was found somewhere between point 4 and 6 within approximately 10 µm. The pressures calculated for points 4, 5 and 6 differ only 0.2 GPa, therefore indicating that the spin transition happened over a very small pressure range.

Finally we note that a more detailed analysis of the collected Raman spectra of DAC-A and DAC-N revealed an abrupt increase in the full width at half maximum (FWHM) of the ν_1-mode upon the HS-LS transition in both of our single-crystal studies (DAC-A and DAC-N). Possible reasons behind this pressure induced FWHM broadening in the non-magnetic LS state might be (a) local stresses (we mention though that the FWHM remains rather constant upon further compression, hence this extrinsic effect can most likely be excluded), (b) local structural disorder, inhomogeneities, defects, and/or (c) a modified vibrational density of states in the LS state, which could lead to a reduction of the respective ν_1 phonon lifetime, i.e. a FWHM increase of the respective Raman-active mode (e. g. Debernardi et al. 2001). A more detailed discussion of this effect, however, lies beyond the scope of this paper.

Discussion

Gradual versus sharp spin transition with respect to pressure increase

Lavina et al. (2010) studied a natural siderite with a near endmember composition using single crystal XRD, observing a sharp, volume collapse of the unit cell volume from HS to LS, without a change in crystalline symmetry. At ca. 45 GPa Lavina et al. (2010) observed a Bragg peak splitting, which was explained as HS and LS domains forming as a consequence of the ongoing spin transition. As their sample size was 12x17 μm^2 and the X-ray spot dimensions either 5x5 or 5x10 μm^2, it is very likely that a large part of the sample is measured in a single measurement. Therefore, if the spin transition occurred over a broad pressure range, they should have been able to observe both HS and LS domains during the spin transition. However, Cerantola et al. (2015) argue that XRD is a technique only sensitive to long-range features. Hence, short-range features such as HS and LS micro-domains should not be observable. Raman spectroscopy should be able to detect such small scale features, which is why in previous Raman studies, the splitting of the ν_1-mode into HS and LS components over a pressure range was assigned to HS and LS microdomains (Spivak et al. 2014, Cerantola et al. 2015).

We observed the spin transition over a pressure range in a siderite film (DAC-A), thus, implying a more gradual change from HS to LS. But this is easily explained by local strain maxima and minima at the grain boundaries (e.g. Takemura 2001; Glazyrin et al. 2016). Therefore, groups of crystals might show the spin transition while others not. With as single measurement signal from several small crystals of different orientations is collected. In contrast, the natural siderite crystal in DAC-N and DAC-A both change rapidly as indicated by the sudden shift of the ν_1-mode to lower frequencies.

In the single crystals in DAC-A and DAC-N the spin transition is accompanied by a color change from transparent to green. In experiment DAC-A we observe a single HS and a single LS domain at the same time (Fig. 10 and 11), which would mean that there is a stress variation in the sample of probably up to 7 GPa based on the results of Spivak et al. (2014) and Cerantola et al. (2015). But by measuring Raman spectra along the crystal we do not observe a large shift of the modes frequencies and, thus, we can rule out a large stress gradient and a spin transition over a wide pressure range. It appears that one either measures a material that is completely HS or completely LS. Looking at Figs. 11 and 12 one may get the impression of coexisting HS and LS siderite domains in a range of pressures. However, this effect is readily explained by the finite spatial resolution at which we measured Raman scattering in our experiments. When getting closer to the transition front, one logically obtains more signal from the other side of the transition front. Cerantola et al. (2015) did observe a color change but no transition front. If they could not distinguish between a single HS and a single LS domain in their crystal there is a possibility of mixed measurements and, thus, they might obtain the impression of a gradual spin transition.

Because of the bridging rubies there is an overestimation of the transition pressure of DAC-A. Thus, the linear regression obtained in DAC-N can only be used to calculate pressure or stress differences within the sample rather than calculating absolute experimental pressure. Nonetheless we could show that over the transition front the calculated stress changes only by 0.2 GPa, which is below our stress/pressure resolution. Consequently, we state that the spin transition in siderite is sharp.

Implications

We were able to quantify the stress variation on the sample in a very precise and self-consistent manner, by employing the calibrated Raman mode frequency as a function of pressure. At ambient temperature we could clearly show that the spin transition in siderite is sharp. Regarding the effect of temperature on the spin transition, for magnesiosiderite Liu et al. (2014) report a broadening of the spin transition from 4 GPa at ambient temperature to 10 GPa at 1200 K. To check whether this broadening is an effect of the spin transition or caused by internal stresses, one could apply the method here described.

In terms of geological significance, siderite may serve as an analog to the major constituents of the Earth's mantle, bridgmanite and ferropericlase, which also undergo spin transitions under high pressure (Badro et al. 2003; Lin et al. 2012). Therefore, by carefully analyzing the stress state on these samples, it should be checked how sharp the spin transition actually is. For the further understanding of Earth's mantle it is important to know whether spin transitions are sharp or broad, since mantle properties like seismic velocities, electrical conductivity, and fractionation processes are directly affected.

Acknowledgements

We thank Michail Taran for providing the natural siderite crystals and Alexandra Friedrich and Björn Winkler for providing the Boehler-Almax DAC and diamonds. Alexandra Friedrich is especially to be thanked for the help with the loading of the DAC. We also thank Max Wilke for providing the siderite powder and Hans-Josef Reichmann for giving valuable advice on experimental questions. This work is part of the DFG funded research group FOR2125 CarboPaT (KO1260/16, JA 1469/9).

294 **References cited**

295

296 Badro, J., Fiquet, G., Guyot, F., Rueff, J.P., Struzhkin, V.V., Vankó, G. and Monaco, G.
297 (2003) Iron partitioning in Earth's mantle: Toward a deep lower mantle discontinuity, Science,
298 300, 789-791.

299

300 Boehler, R. (2006) New diamond cell for single-crystal x-ray diffraction, Reviews of
301 Scientific Instruments 77, 115103.

302

303 Cerantola, V., McCammon, C., Kupenko, I., Kantor, I., Marini, C., Wilke, M., Ismailova, L.,
304 Solopova, N., Chumakov, A., Pascarelli, S. and Dubrovinsky, L. (2015) High-pressure
305 spectroscopic study of siderite ($FeCO_3$) with focus on spin crossover, American Mineralogist,
306 100, 2670-2681.

307

308 Debernardi, A., Ulrich, C., Cardona, M. and Syassen, K. (2001) Pressure Dependence of
309 Raman Linewidth in Semiconductors, Physica Status Solidi (b), 223, 213-223.

310

311 Farfan, G., Wang , S., Ma, H., Caracas, R. and Mao, W.L. (2012) Bonding and structural
312 changes in siderite at high pressure, American Mineralogist, 97, 1421-1426.

313

314 French, B.M. (1971) Stability relations of siderite ($FeCO_3$) in the system Fe-C-O, American
315 Journal of Science, 27, 37-78.

316

317 Glazyrin, K., Miyajima, N., Smith, S.S. and Lee, K.K.M. (2016) Compression of a multiphase
318 mantle assemblage: Effects of undesirable stress and stress annealing on the iron spin state
319 crossover in ferropericlase, Journal of Geophysical Research: Solid Earth, 121,
320 doi:10.1002/2015JB012321
321
322 Isshiki, M., Irifune, T., Hirose, K., Ono, S., Ohishi, Y., Watanuki, T., Nishibori, E., Takata, M.
323 and Sakata, M. (2004) Stability of magnesite and its high pressure form in the lowermost
324 mantle, Nature, 427, 60-63.
325
326 Kaminsky, F. (2012) Mineralogy of the lower mantle: a review of 'super-deep' mineral
327 inclusions in diamond, Earth-science Reviews, 110, 127-147.
328
329 Klotz, S., Chervin, J.C., Munsch, P. and Le Marchand, G. (2009) Hydrostatic limits of 11
330 pressure transmitting media, Journal of Physics D, 42, 075413.
331
332 Langille, D.B. and O'Shea, D.C. (1977) Raman spectroscopy studies of antiferromagnetic
333 $FeCO_3$ and related carbonates, Journal of physics and chemistry of solids, 38, 1161-1171.
334
335 Lavina, B., Dera, P., Downs, R.R., Prakapenka, V., Rivers, M., Sutton, S. and Nicol, M.
336 (2009) Siderite at lower mantle conditions and the effects of the pressure-induced spin pairing
337 transition, Geophysical Research Letters, 36, L23306.
338

Lavina, B., Dera, P., Downs, R.T., Yang, W., Sinogeikin, S., Meng, Y., Shen, G. and Schiferl, D. (2010) Structure of siderite $FeCO_3$ to 56 GPa and hysteresis of its spin pairing transition, Physical Review B, 82, 064110.

Lin, J.F., E.E. Alp, Z. Mao, T. Inoue, C. McCammon, Y.M. Xia, P. Chow, and J.Y. Zhao (2012) Electronic spin states of ferric and ferrous iron in the lower-mantle silicate perovskite, American Mineralogist, 97, 592–597.

Lin, J.-F., Speziale, S., Mao, Z. and Marquardt, H. (2013) Effects of the electronic spin transitions of iron in lower mantle minerals: Implications for deep mantle geophysics and geochemistry, Reviews of Geophysics, 51, 244-273.

Liu, J., Lin, J.-F., Mao, Z. and Prakapenka, V.B. (2014) Thermal equation of state and spin transition of magnesiosiderite at high pressure and temperature, American Mineralogist, 99, 84-93.

Lobanov, S.S., Goncharov, A.F., and Litasov, K.D. (2015) Optical properties of siderite ($FeCO_3$) across the spin transition: Crossover to iron-rich carbonates in the lower mantle, American Mineralogist, 100, 1059-1064.

Mao, H.K., Xu, J. and Bell, M. (1986) Calibration of the ruby pressure gauge to 800 kbar under quasi-hydrostatic conditions, Journal of Geophysical Research, 91, 4673.

362 Matilla, A., Pylkkänen, T., Rueff, J-P., Huotari, S., Vanko, G., Hanfland, M., Lehtinen, M. and
363 Hämäläinen, K. (2007) Pressure induced magnetic transition in siderite $FeCO_3$ studied by x-
364 ray emission spectroscopy, Journal of Physics: Condensed Matter, 19, 386206.
365
366 Merlini, M., Hanfland, M. and Crichton, W.A. (2012) $CaCO_3$-III and $CaCO_3$-VI, high pressure
367 polymorphs of calcite: possible host structures for carbon in the Earth's mantle, Earth and
368 Planetary Science Letters, 333-334, 265-271.
369
370 Nagai, T., Ishido, T. Seto, Y., Nishio-Hamane, D., Sata, N. and Fujino, K. (2010) Pressure-
371 induced spin transition in $FeCO_3$-siderite studied by X-ray diffraction measurements, Journal
372 of Physics: Conference Series, 215, 012002.
373
374 Rutt, H.N., Nicola, J.H. (1974) Raman spectra of carbonates of calcite structure, Journal of
375 Physics C: Solid State Physics, 7, 4522-4528.
376
377 Spivak, A., Solopova, N., Cerantola, V., Bykova, E., Zakharchenko, E., Dubrovinsky, L. and
378 Litvin, Y. (2014) Raman study of $MgCO_3$-$FeCO_3$ carbonate solid solution at high pressure up
379 to 55 GPa, Physics and Chemistry of Minerals, 41, 633-638.
380
381 Takemura, K. (2001) Evaluation of the hydrostaticity of a helium-pressure medium with
382 powder x-ray diffraction techniques, Journal of Applied Physics, 89, 662.
383
384

This is a preprint, the final version is subject to change, of the American Mineralogist (MSA)
Cite as Authors (Year) Title. American Mineralogist, in press.
(DOI will not work until issue is live.) DOI: http://dx.doi.org/10.2138/am-2016-5708

385

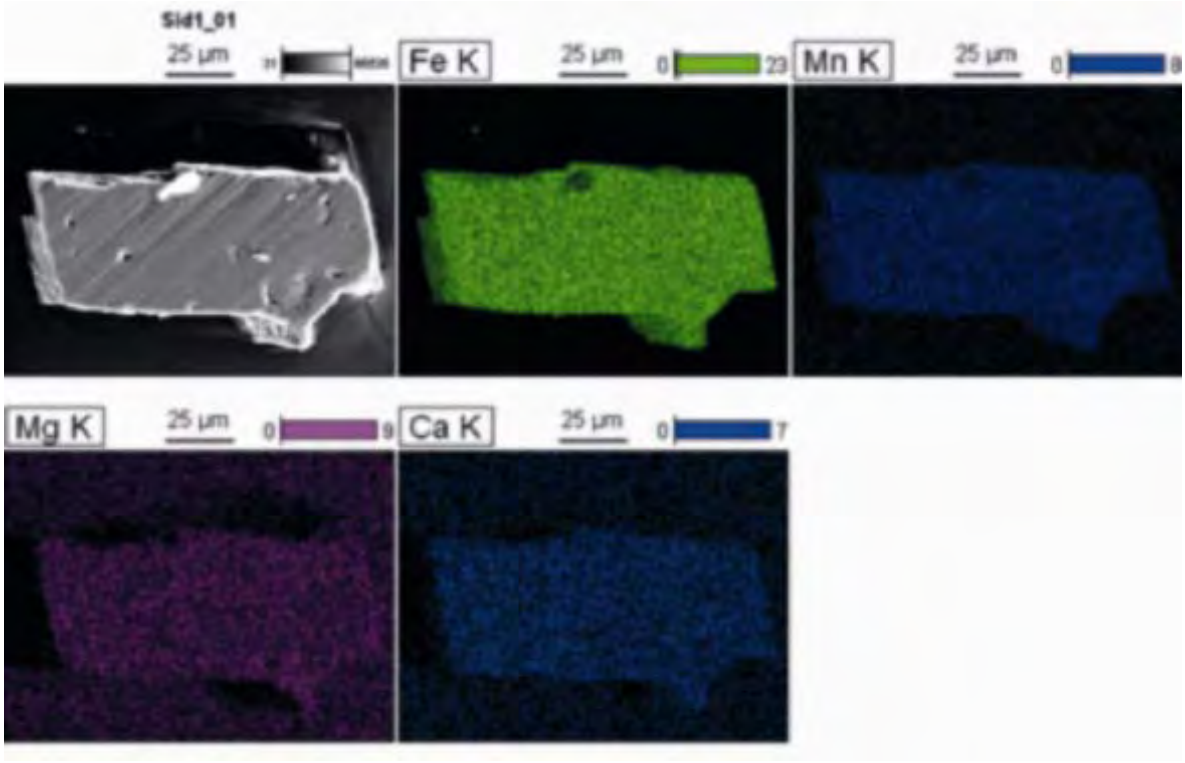

386

387 **Figure 1.** SEM mapping of a representative natural siderite crystal showing that the four main
388 components Fe, Mn, Mg and Ca are all homogeneously distributed within the crystal. At the
389 upper side of the crystal some dirt is found. The stripes are caused by polishing of the crystal.

390

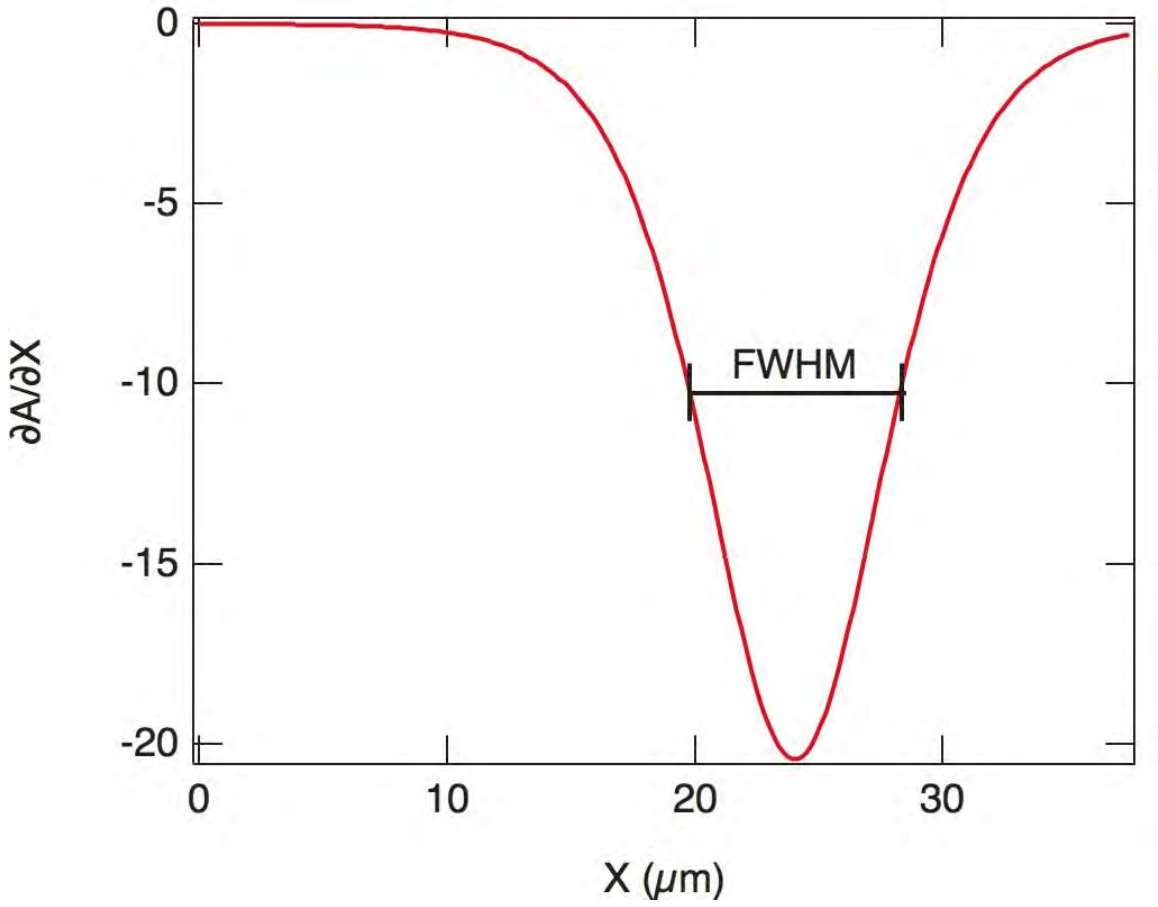

Figure 2. The change of amplitude with respect to change of the position on a crystal is plotted against the position on the crystal. The FWHM (9±1 μm) gives the spatial resolution of our Raman experiments.

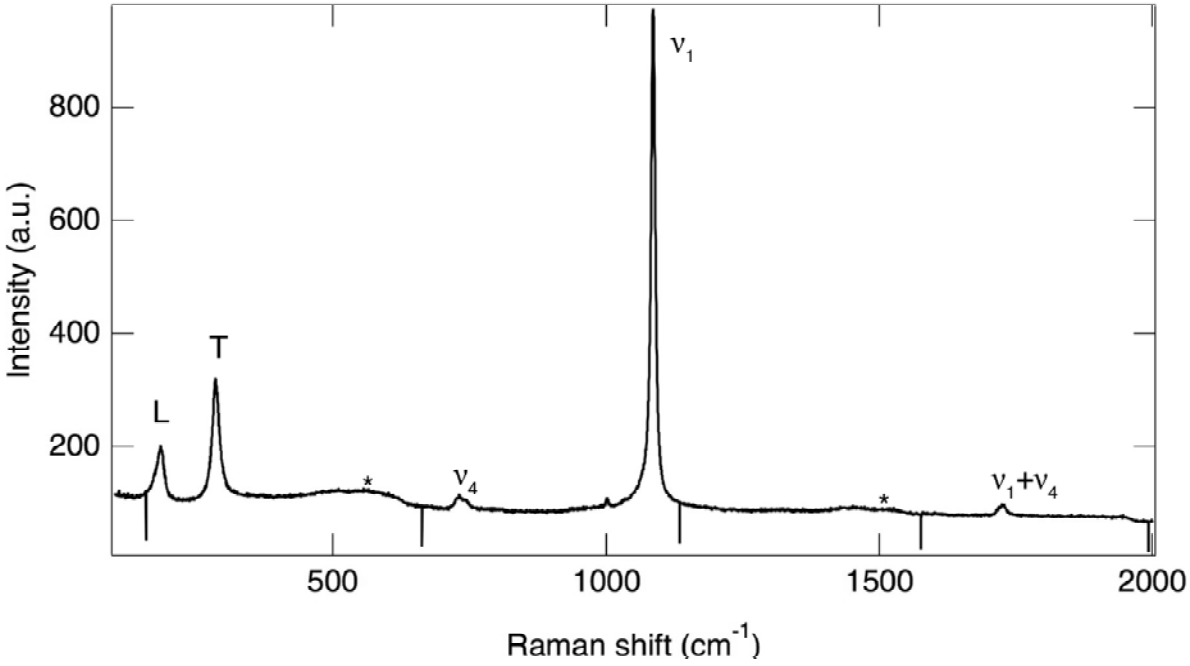

Figure 3. Raman spectra of a natural siderite single crystal between 100 and 2000 cm^{-1} at ambient conditions.

This is a preprint, the final version is subject to change, of the American Mineralogist (MSA)
Cite as Authors (Year) Title. American Mineralogist, in press.
(DOI will not work until issue is live.) DOI: http://dx.doi.org/10.2138/am-2016-5708

413

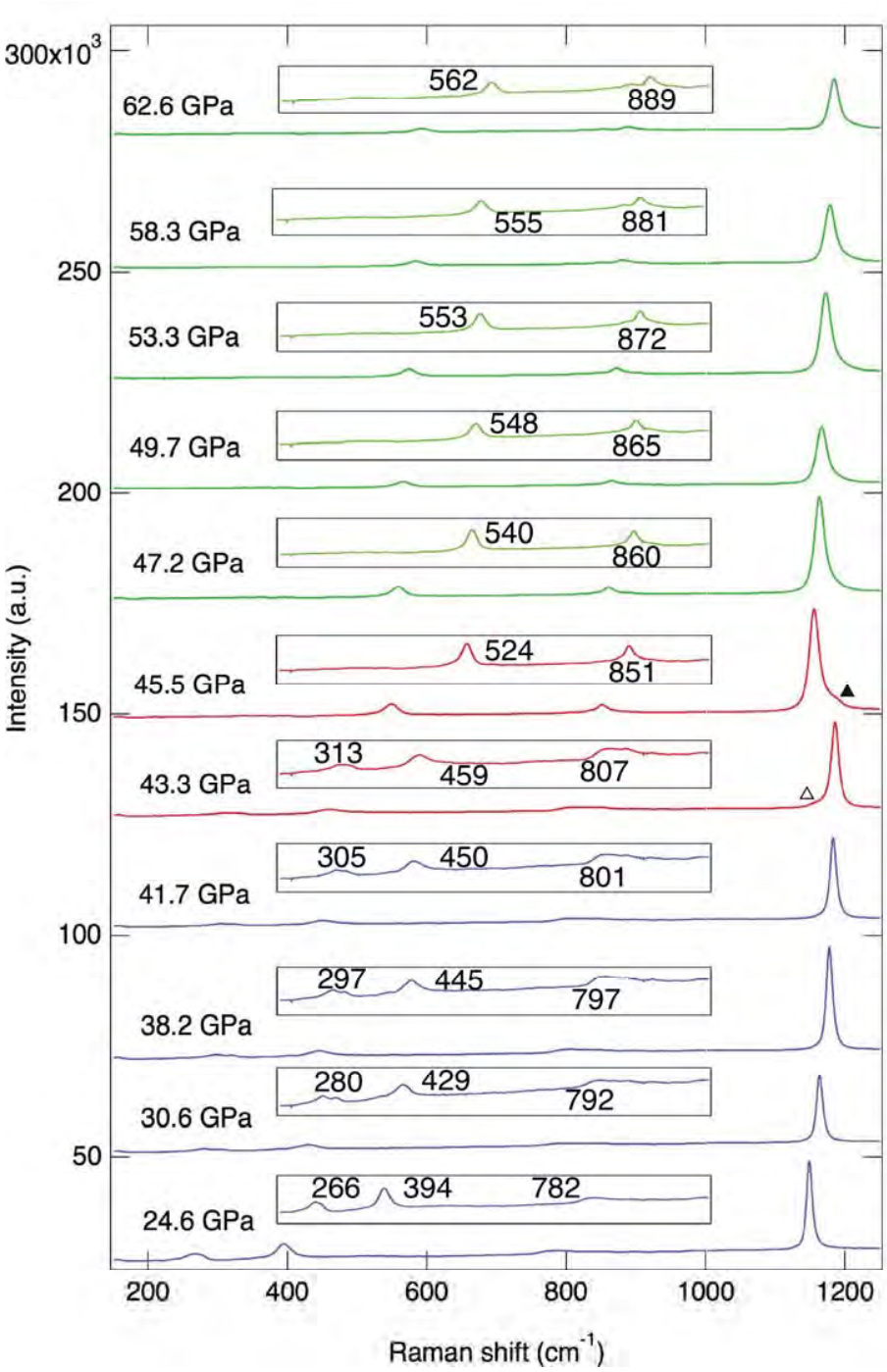

414

415 **Figure 4**. Raman spectra of DAC-N. Blue spectra show HS siderite, red spectra show a
416 transition area from HS to LS and green spectra show LS siderite. At 43.3 GPa the empty

417 triangle marks the occurrence of a small shoulder, which belongs to the first occurring LS
418 siderite and at 45.5 GPa the black triangle marks the last remaining HS siderite. The range of
419 the magnification is from 200 to 1000 cm^{-1}.

420
421

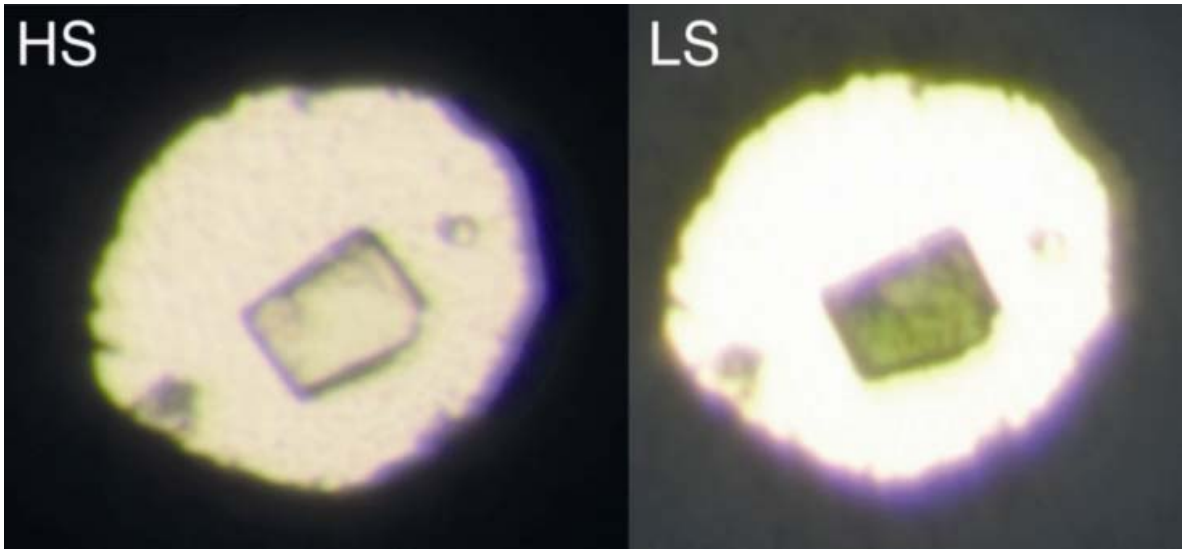

422

423 **Figure 5.** Picture of the single crystal of DAC-N. In the HS-state the crystal is transparent and
424 in the LS-state it turns green.

425
426
427
428
429

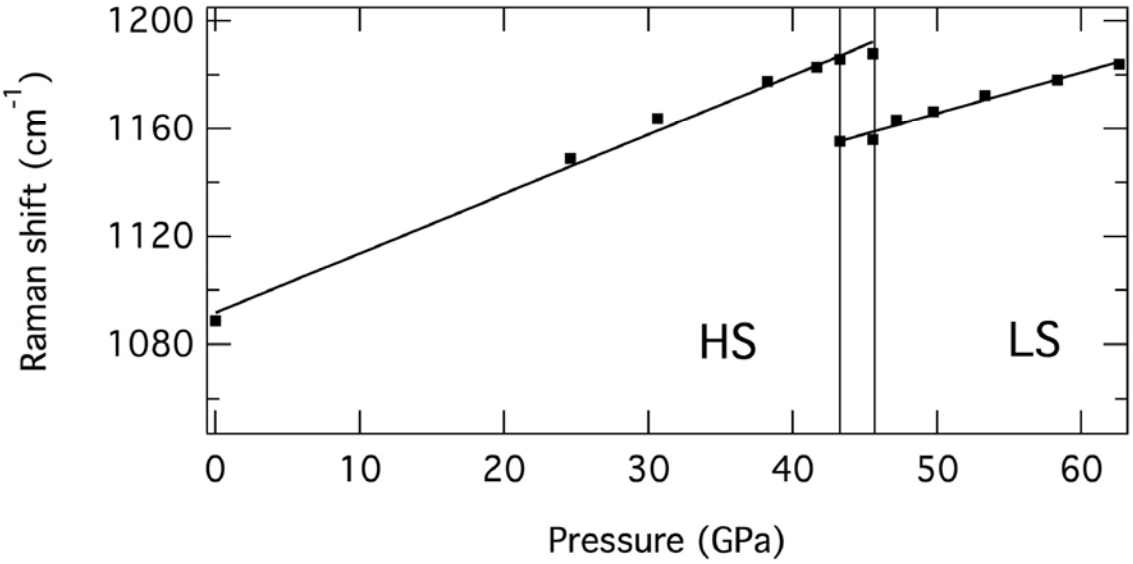

Figure 6. Raman shift of the ν_1-mode measured in neon plotted against pressure. With increasing pressure the ν_1-mode moves to higher frequencies. At ca. 43.3 GPa the LS ν_1-mode appears at lower wavenumbers and at 45.5 the HS ν_1-mode is nearly gone. The black lines are the linear fits for either the HS or the LS ν_1-mode.

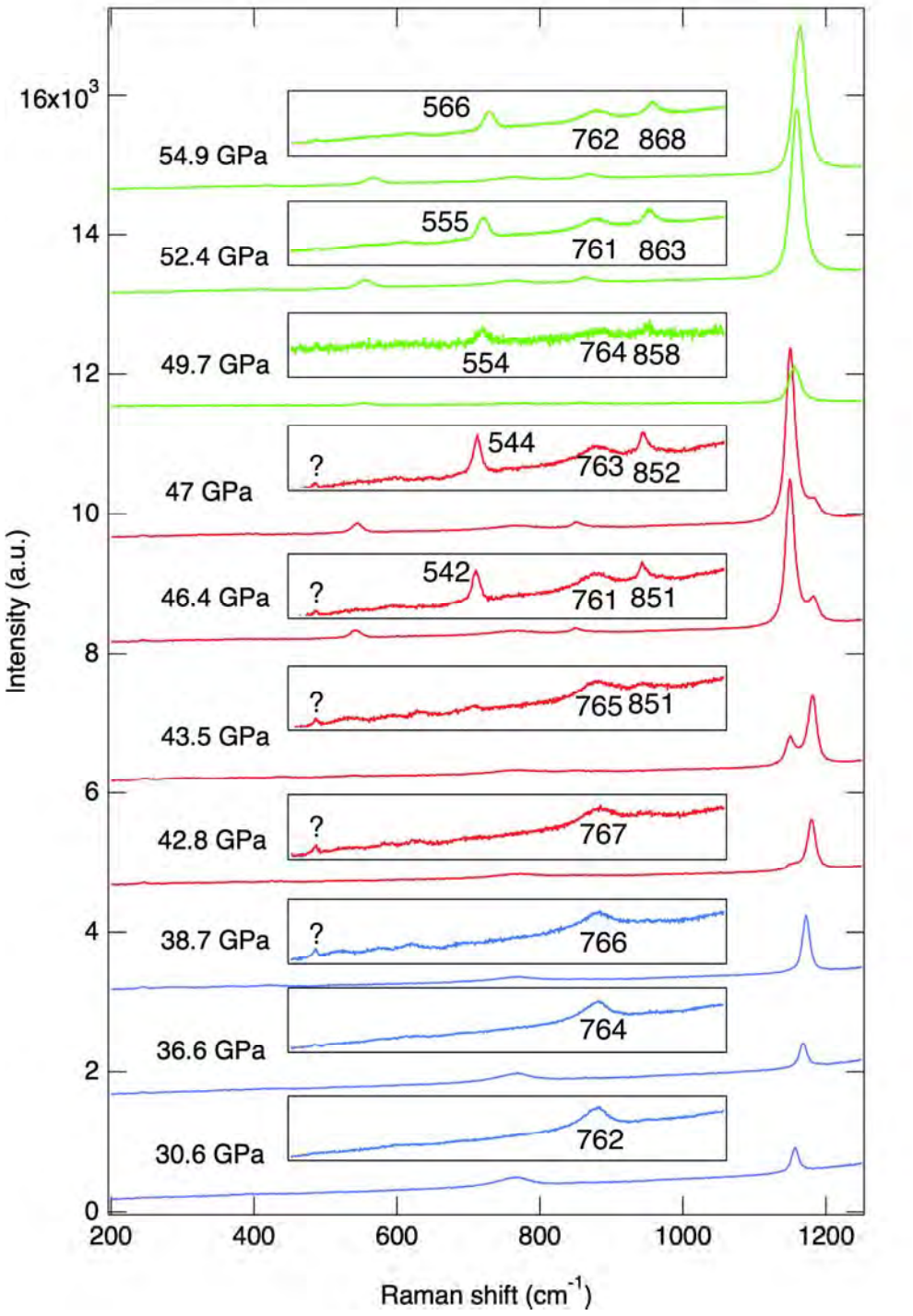

Figure 7. Raman spectra (DAC-A) of a film of pure siderite measured from 30.6 to 54.9 GPa. Blue spectra show HS siderite, red spectra show a transition area from HS to LS and green

445 spectra show LS siderite. The signal at 760 cm^{-1} is an artifact, which does not belong to the
446 sample. The range of the magnification is from 200 to 1000 cm^{-1}.

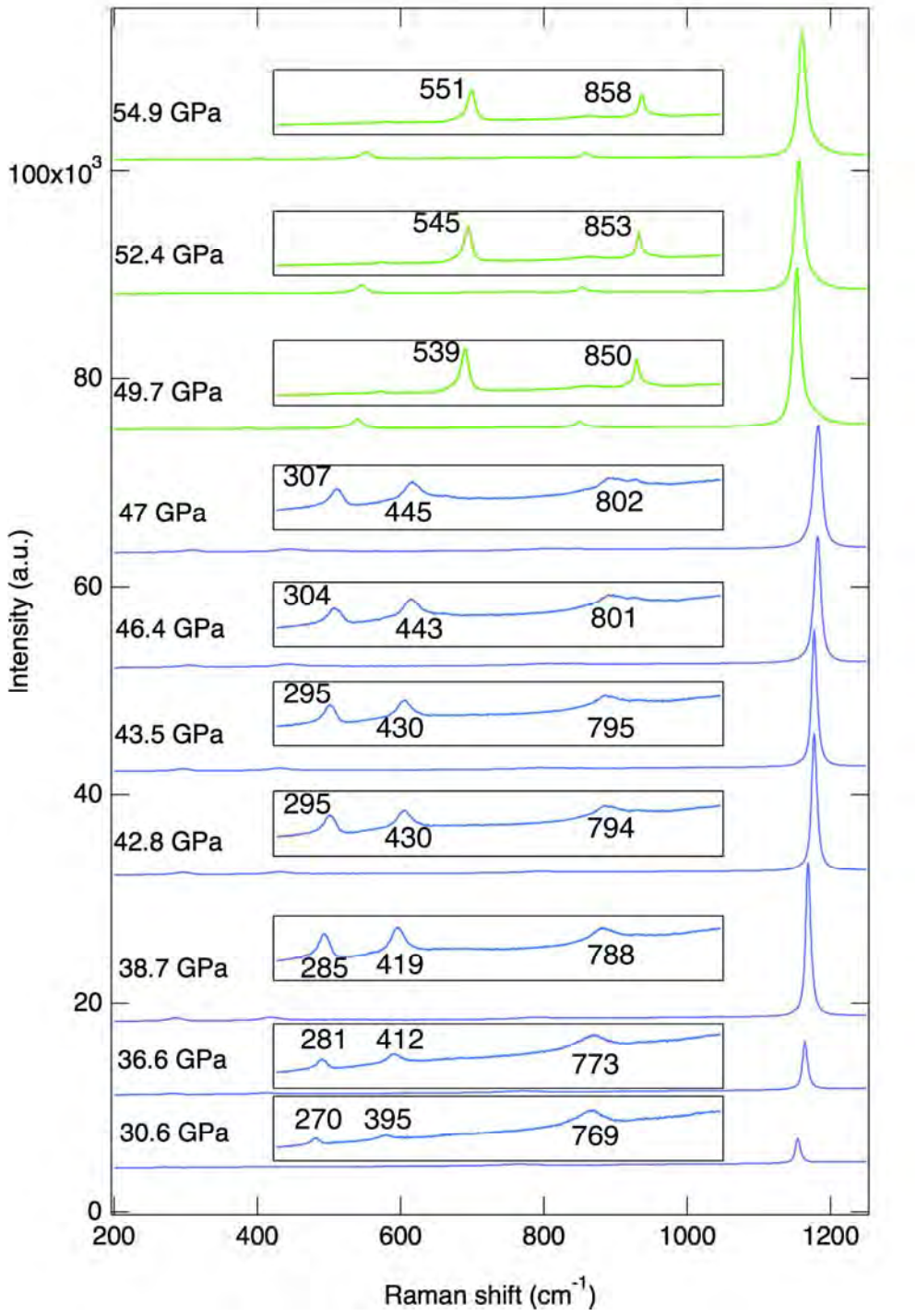

Figure 8. Raman spectra (DAC-A) of a natural siderite crystal measured from 30.6 to 54.9 GPa. Blue spectra show HS siderite and green spectra show LS siderite. The range of the magnification is from 200 to 1000 cm^{-1}.

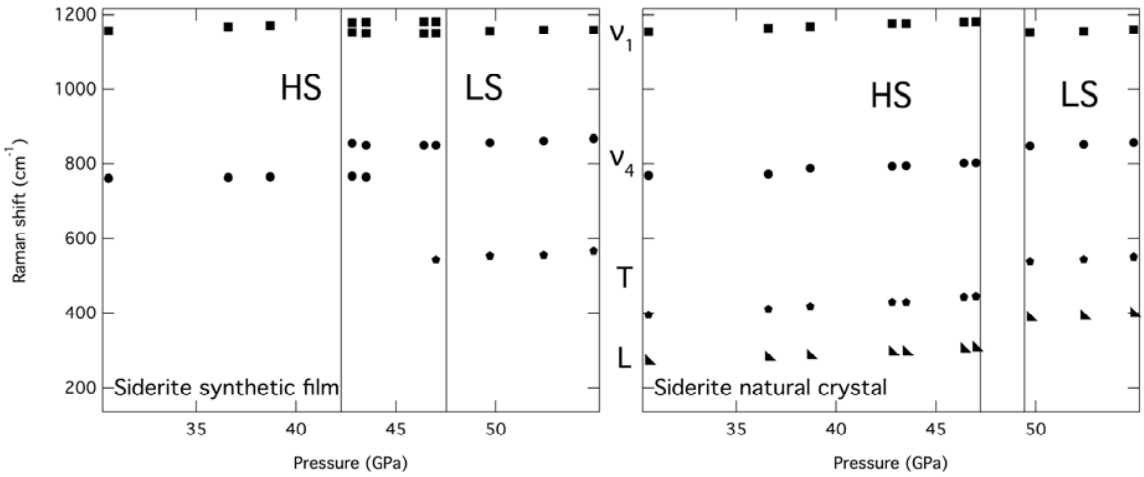

Figure 9. Raman shift of the observed modes plotted against pressure for the siderite film (left) and the siderite single crystal (right). The plotted results are measured under compression. The pressure region where the spin transition is observed is marked by the vertical black lines.

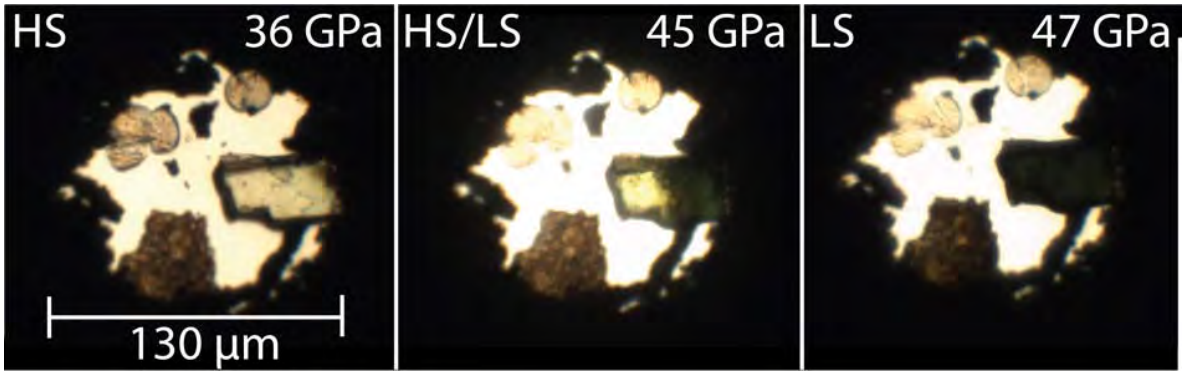

Figure 10. View of the sample chamber at 36, 45, and 47 GPa. At the top are the round and fractured rubies, at the bottom is the brown siderite film and at the right side is the natural siderite single crystal. The black parts are dirt from the rhenium gasket. At 36 GPa the crystal

462 is transparent and in the HS state, at 45 GPa during decompression half of the crystal is
463 transparent (HS) and half is green (LS). At 47 GPa the crystal is completely dark green and
464 therefore in the LS-state.

465

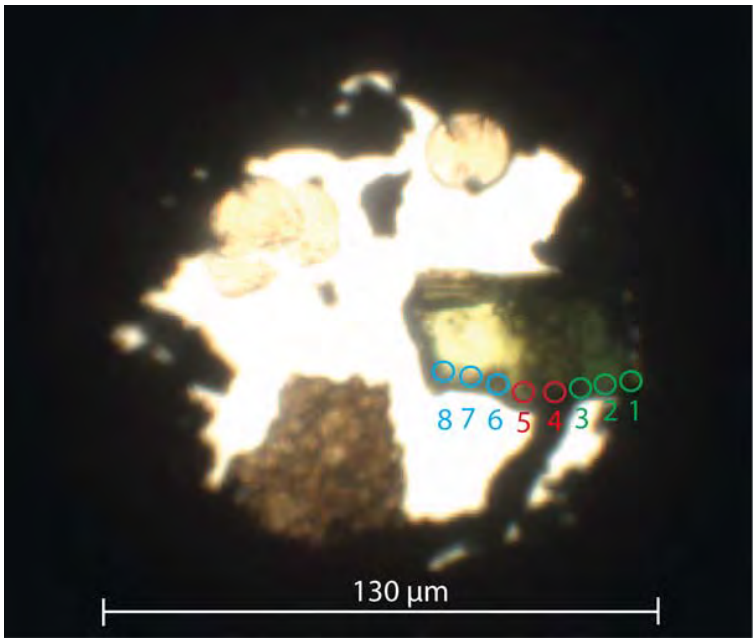

466

467 **Figure 11.** Measurement points where Raman spectra were taken at approximately 45 GPa.
468 Blue is on the HS side, red is on the border of HS and LS and green is on the LS side.

469

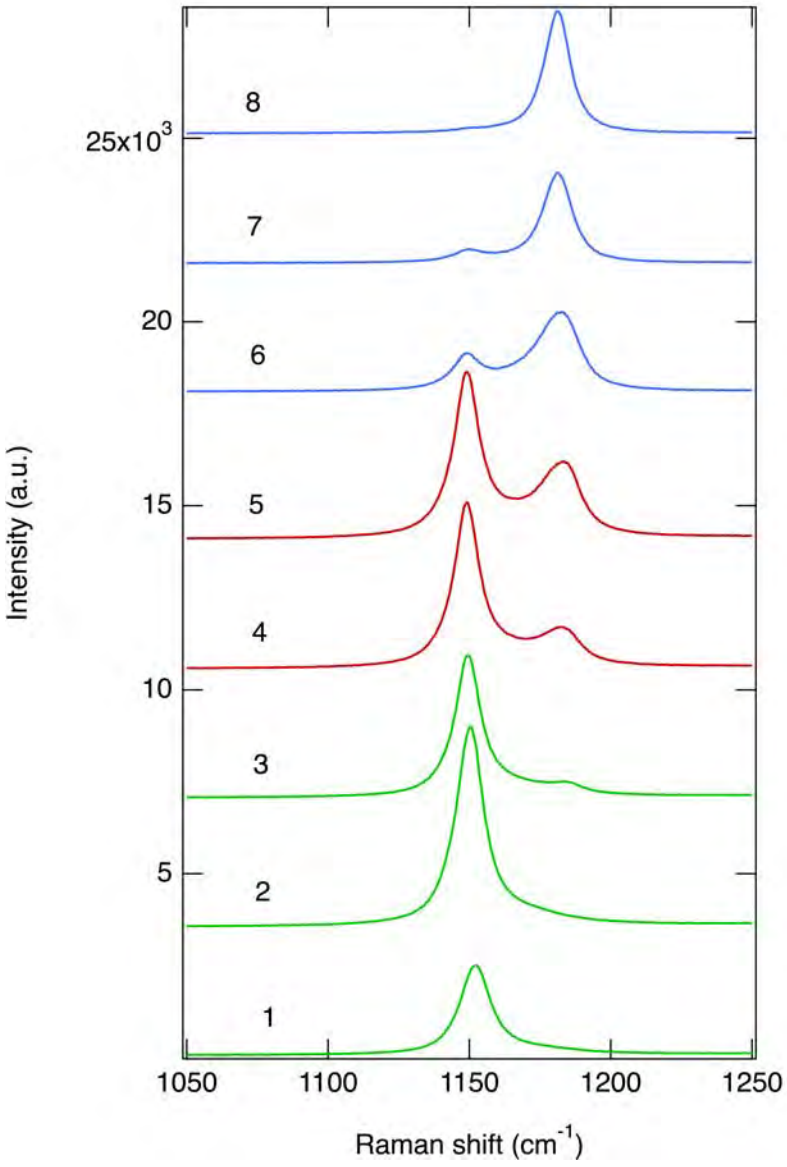

Figure 12. Raman spectra at 45 GPa during decompression showing the ν_1-mode belonging to the measurement points in Fig. 11. Blue is in the HS state, red is on the border and shows HS and LS and green is in the LS-state. The closer the measurements get to the transition front, the more are the measurements mixed.

Table 1. Overview of the current literature about siderite and a comparison of their used methods, composition and transition pressure.

Reference	Method	Pressure transmitting medium	Spot size [µm²]	Sample size [µm²]	Composition	Transition pressure [GPa]
Cerantola et al. (2015)	Raman	Neon	2 x 2	15 x 15	$FeCO_3$	40 – 47
Lobanov et al. (2015)	UV-VIS	Neon	50 x 50	30 x 50	$Fe_{0.95}Mn_{0.05}CO_3$	43 – 45
Spivak et al. (2014)	Raman	Neon	2 x 2	15 x 15	$FeCO_3$	40 – 47
Liu et al. (2014)	Powder + single crystal XRD	Neon	N/A	N/A	$Fe_{0.65}Mg_{0.33}Mn_{0.02}CO_3$	43 to 47 (single crystal XRD)
Farfan et al. (2012)	XRD + Raman	None (XRD); silicone oil (Raman)	2 x 2 (Raman)	N/A	$Fe_{0.76}Mn_{0.15}Mg_{0.09}Ca_{0.01}CO_3$	46 (XRD); 46 – 50 (Raman)
Lin et al. (2012)	Powder + single crystal XRD + Raman	Neon	~ 5 (XRD);	45 x 50 Raman	$Fe_{0.65}Mg_{0.33}Mn_{0.02}CO_3$	45
Nagai et al. (2010)	Powder XRD	Argon	N/A	N/A	N/A	47 – 50
Lavina et al. (2010)	Single crystal XRD	Neon	5 -10 x 5 - 10	12 x 17	Near endmember	44 – 45
Mattila et al. (2007)	XES	Argon; None above 40 GPa	120 x 55	N/A	$Fe_{0.96}Mn_{0.04}CO_3$	~ 50

Table 2. Raman peak positions of the ν_1-mode measured in argon and their respective calculated pressures and deviations. Point 1 is the reference point for ΔP LS and point 3 for ΔP HS.

Point	LS ν_1 [cm^{-1}]	HS ν_1 [cm^{-1}]	P LS [GPa]	P HS [GPa]	ΔP LS [GPa]	ΔP HS [GPa]
1	1152.0	-	41	-	0	-
2	1150.2	-	39.9	-	1.1	-
3	1149.0	1182.8	39.1	41.3	1.9	0
4	1149.0	1183.0	39.1	41.4	1.9	-0.1
5	1149.0	1183.4	39.1	41.5	1.9	-0.2
6	1149.4	1183.4	39.3	41.5	1.7	-0.2
7	1150.1	1181.1	39.8	40.5	1.2	0.8
8	-	1181.0	-	40.5	-	0.8